31st Youth Academic Annual Conference of Chinese Association of Automation
Wuhan, China; November 11-13, 2016

Modeling and Motion Control of Self-Balance Robots on the Slope

Dingkun Liang, Ning Sun*, Yiming Wu, and Yongchun Fang
Institute of Robotics and Automatic Information System, Tianjin Key Laboratory of Intelligent Robotics
Nankai University
Tianjin, 300353, China
Email: liangdk@mail.nankai.edu.cn; sunn@nankai.edu.cn; ymwu@mail.nankai.edu.cn; fangyc@nankai.edu.cn

***Abstract*—As a typical underactuated system, the two-wheeled self-balance robot (TWSBR) is similar to the wheeled inverted pendulum in structure. There have been plenty of studies about TWSBRs operated on the horizontal plane; however, sometimes TWSBRs need to move on non-flat ground, e.g., slopes. To tackle the control problem of TWSBRs when they move on an inclined slope, the dynamic model of TWSBRs on the slope is established in this paper. Then, the equilibrium point of the system is analyzed, and the system dynamics are expressed in the state space form. Further, the linear quadratic regulator (LQR) method is used to design a linear controller. Finally, to validate the effectiveness of the proposed controller, numerical simulation results are presented.**

Keywords—self-balance robots; underactuated systems; modeling

I. INTRODUCTION

The mobile robot is an intelligent robotic device which can execute a lot of tasks. The Stanford Research Institute developed the first mobile robot—Shakey in the 1960s [1]. However, the process of trajectory planning always costs Shakey few hours due to the poor calculating performance of the computer in the 1960s. Nowadays, with the rapid development of science and technology, mobile robots of many other companies are completely different from those in Shakey's time.

The two-wheeled self-balance robot (TWSBR) is a kind of control system to keep balance during the transport process. It is traditionally simplified as a wheeled inverted pendulum system (WIPS). The WIPS is a typical underactuated system, like many other mechatronic systems, says, e.g. [2]-[12]. Many ambitious works have been done in this area. Yamafuji *et al.* put forward a control approach for TWSBR by using the gain changing technique and the servo-reference method to control the rotation of each wheel [13]. Segway LLC invents a new type of two-wheeled balanced vehicle called Segway [14], which uses five gyroscopes and a series of sensors to keep balance and can be steered by changing the center of gravity of the driver. LEGO also designs a self-balance robot named as Legway [15], it can be assembled and separated easily and can also adjust its equilibrium points during the moving process.

This work is supported by the National Natural Science Foundation of China under Grant 61503200, the Natural Science Foundation of Tianjin under Grant 15JCQNJC03800, and the Fundamental Research Funds for the Central Universities. *(Corresponding Author: Ning Sun.)*

Currently, in the literature, most of the studies are carried out based on the model of the TWSBR on the horizontal plane. Do *et al*. combine nested p-times differentiable saturation and backstepping techniques to design a control law for the TWSBR on the horizontal plane in [16]. To improve the performance, Katariya designs optimal state-feedback and output-feedback controllers for the wheeled inverted pendulum system in [17]. More recently, Xu *et al.* present an integral sliding mode controller (ISMC) on a single wheel mobile robot's model and consider the tilt angle of inclined plane in [18].

In practical applications, TWSBRs are often required to drive on non-flat planes, e.g., on the slope. However, most of the existing works only consider the dynamics of TWSBRs on the horizontal plane. In this paper, we are interested in modeling and control of TWSBRs on the slope. For the TWSBR system, the control objective is to control the tilt angle of the pendulum, the yaw angle of the chassis, and the displacement of the vehicle at the same time by properly outputting the torques of the wheels. To do so, this paper sets up the dynamic model of TWSBRs on the slope. Then, we design an LQR controller to achieve the control objective for TWSBRs on the slope. At last, some numerical simulation results are included for verification.

The rest of this paper is organized as follows. The dynamics of TWSBRs on the slope are described in Section II. The dynamics are expressed in the state space form in Section III. We present some simulation results with MATLAB/Simulink and validate the effectiveness of the proposed controller in Section IV. The main work of this paper is finally summarized in Section V.

II. MODELING OF TWSBRS ON THE SLOPE

A. Simplified Model of TWSBR Systems

The TWSBR system has a body above two wheels with no balancing support and with an inverted pendulum connected with the chassis. It consists of two wheels, power mechanisms, a chassis, an inverted pendulum and control units. The TWSBR is a typical underactuated system. We build the dynamics by using the right hand coordinate system. In this paper, the dynamic model of the TWSBR system on the slope, as shown in Fig. 1 is given. The schematic illustration of the left and right wheels with all relevant forces and accelerations labeled is

978-1-5090-4423-8/16/$31.00 ©2016 IEEE

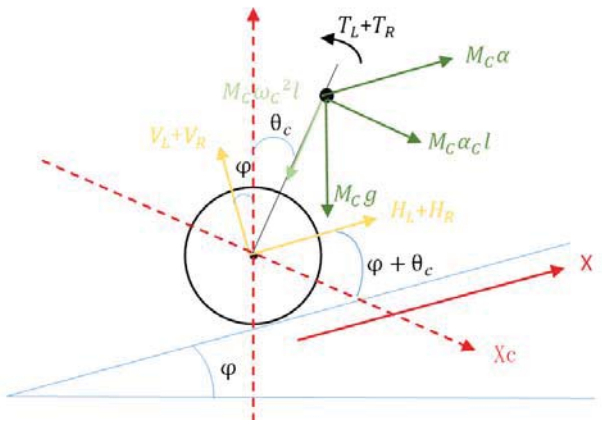

Fig. 1. The schematic model of the TWSBR system.

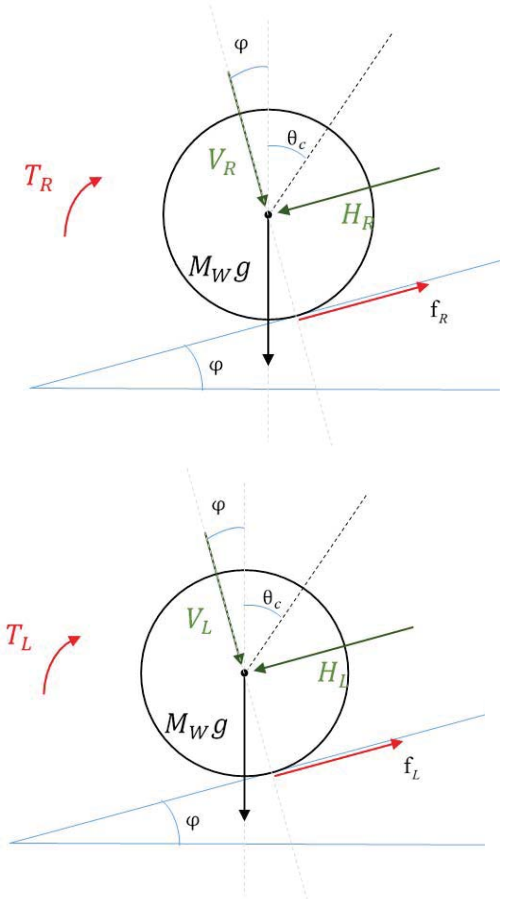

Fig. 2. The schematic model of the left/right wheel.

TABLE I. VEHICLE PARAMETERS AND VARIABLES

Variable name	meaning
M_W	Mass of each wheel
M_C	Mass of the chassis
H_L, H_R	Horizontal relation force between the chassis and the left/right wheel
V_L, V_R	Vertical relation force between the chassis and the left/right wheel
T_L, T_R	Torque of the wheels
f_L, f_R	Friction of the left/right wheel
X	The vehicle displacement
θ_C	Tile angle of the inverted pendulum
δ	Yaw angle of the chassis
φ	Tilt angle of the slope
α, α_C	Accelerations of the pendulum on different directors
ω_C	Angular velocity of the inverted pendulum
l	Distance about the center of gravity of pendulum
g	Acceleration of gravity
r	Radius of each wheel
d	Distance between the two wheels
I_W	Moment of inertia of each wheel
I_Y, I_C	Moment of inertia of the chassis about the Y/Z axis
θ_{WL}, θ_{WR}	Rotation angle for the left/right wheel
X_L, X_R	Displacement of the left/right wheel

shown in Fig. 2. The definitions of the parameters and variables are given in Table I.

B. Lagrangian Approach

The first step in deriving the equations of motion using the Lagrangian method is to derive the Lagrangian $\mathcal{L}$, which is given by

$$\mathcal{L}=T-V$$

where T and V are the total kinetic energy and potential energy of the system, respectively. From Fig. 2, the translational kinetic energy of the chassis can first be derived as follows:

$$\begin{aligned}&\frac{1}{2}M_C\left[\left(\dot{X}+l\dot{\theta}_C\cos\left(\theta_C+\varphi\right)\right)^2+\left(-l\dot{\theta}_C\sin\left(\theta_C+\varphi\right)\right)^2\right]\\&=\frac{1}{2}M_C\left[\dot{X}^2+2\dot{X}l\dot{\theta}_C\cos\left(\theta_C+\varphi\right)+l^2\dot{\theta}_C{}^2\right]\end{aligned}\quad(1)$$

The translational kinetic energies of the left and right wheels are

$$\frac{1}{2}M_W\dot{X}_L^{\,2},\frac{1}{2}M_W\dot{X}_R^{\,2}$$

The rotational kinetic energy of the chassis is $\frac{1}{2}I_C\dot{\theta}_C^{\,2}$. The rotational kinetic energies of the left and right wheels are

$$\frac{1}{2}I_W\dot{\theta}_{WL}^{\,2}=\frac{1}{2}\frac{I_W}{r^2}\dot{X}_L^{\,2},\frac{1}{2}I_W\dot{\theta}_{WR}^{\,2}=\frac{1}{2}\frac{I_W}{r^2}\dot{X}_R^{\,2}$$

The total kinetic energy can be written into the following form:

$$\begin{aligned}T=&\frac{1}{2}M_W\left(\dot{X}_L^{\,2}+\dot{X}_R^{\,2}\right)+\frac{1}{2}\frac{I_W}{r^2}\left(\dot{X}_L^{\,2}+\dot{X}_R^{\,2}\right)\\&+\frac{1}{2}M_C\left[\dot{X}^2+2\dot{X}l\dot{\theta}_C\cos\left(\theta_C+\varphi\right)+l^2\dot{\theta}_C^{\,2}\right]+\frac{1}{2}I_C\dot{\theta}_C^{\,2}\end{aligned}\tag{2}$$

Further, by setting the horizontal plane as the zero potential energy surface, we calculate the potential energy of the system as follows:

$$V=M_Cg\left(l\cos\theta_C+X\sin\varphi\right)+2M_WgX\sin\varphi\tag{3}$$

The Lagrangian $\mathcal{L}$ can be represented by

$$\begin{aligned}\mathcal{L}=&\frac{1}{2}\left(M_W+\frac{I_W}{r^2}\right)\left(\dot{X}_L^{\,2}+\dot{X}_R^{\,2}\right)+\frac{1}{2}M_C\dot{X}^2\\&+\frac{1}{2}\left(M_Cl^2+I_C\right)\dot{\theta}_C^{\,2}+M_C\dot{X}l\dot{\theta}_C\cos\left(\theta_C+\varphi\right)\\&-M_Cg\left(l\cos\theta_C+X\sin\varphi\right)-2M_WgX\sin\varphi\end{aligned}\tag{4}$$

Now, based on the forces acting on the left and right wheels shown in Fig. 3, the equations of motion for the left and the right wheels are computed respectively as follows:

$$\begin{aligned}&\frac{d}{dt}\frac{\partial\mathcal{L}}{\partial\dot{X}_L}-\frac{\partial\mathcal{L}}{\partial X_L}=\frac{T_L}{r}-H_L\rightarrow\left(M_W+\frac{I_W}{r^2}\right)\ddot{X}_L=\frac{T_L}{r}-H_L\\&\frac{d}{dt}\frac{\partial\mathcal{L}}{\partial\dot{X}_R}-\frac{\partial\mathcal{L}}{\partial X_R}=\frac{T_R}{r}-H_R\rightarrow\left(M_W+\frac{I_W}{r^2}\right)\ddot{X}_R=\frac{T_R}{r}-H_R\end{aligned}\tag{5}$$

Then, by inserting the $2\ddot{X}=\ddot{X}_L+\ddot{X}_R$ into Eq. (5) and making some arrangements, we can obtain the following conclusion:

$$2\left(M_W+\frac{I_W}{r^2}\right)\ddot{X}=\frac{T_L+T_R}{r}-\left(H_L+H_R\right)\tag{6}$$

The equation of motion for the chassis displacement is

$$\frac{d}{dt}\frac{\partial\mathcal{L}}{\partial\dot{X}}-\frac{\partial\mathcal{L}}{\partial X}=\left(H_L+H_R\right)\tag{7}$$

From Eqs. (1)-(7), the first equation of the system dynamics can be obtained as follows:

$$\begin{aligned}\left(2M_W+M_C+\frac{2I_W}{r^2}\right)\ddot{X}=&\frac{T_L+T_R}{r}-M_Cl\ddot{\theta}_C\cos\left(\theta_C+\varphi\right)\\&-\left(M_C+2M_W\right)g\sin\varphi\\&+M_Cl\dot{\theta}_C^{\,2}\sin\left(\theta_C+\varphi\right)\end{aligned}\tag{8}$$

Similarly, on the other hand, by taking the derivative of θ_C, we can yield the following equation:

$$\frac{d}{dt}\frac{\partial\mathcal{L}}{\partial\dot{\theta}_C}-\frac{\partial\mathcal{L}}{\partial\theta_C}=-\left(T_L+T_R\right)\tag{9}$$

Hence, by solving Eq. (9), the second equation of system dynamics can be derived as follows:

$$\begin{aligned}\left(M_Cl^2+I_C\right)\ddot{\theta}_C=&-\left(T_L+T_R\right)+M_Cgl\sin\theta_C\\&-M_C\ddot{X}l\cos\left(\theta_C+\varphi\right)\end{aligned}\tag{10}$$

Finally, we consider the rotational motion of the chassis to obtain the yaw angle δ as follows:

$$\left(H_L\text{-}H_R\right)\frac{d}{2}=I_Y\ddot{\delta}\rightarrow\left(H_L\text{-}H_R\right)=\frac{2I_Y\ddot{\delta}}{d}\tag{11}$$

where

$$\ddot{\delta}=\frac{\ddot{X}_L-\ddot{X}_R}{d}\tag{12}$$

Then, from Eqs. (11) and (12), the following conclusion can be obtained:

$$\ddot{\delta}=\frac{\left(T_L-T_R\right)dr}{\left(M_Wd^2r^2+I_Wd^2+2I_Yr^2\right)}\tag{13}$$

Hence, the dynamics of TWSBRs on the slope are derived as follows:

$$\begin{aligned}\left(2M_W+M_C+\frac{2I_W}{r^2}\right)\ddot{X}=&\frac{T_L+T_R}{r}-M_Cl\ddot{\theta}_C\cos\left(\theta_C+\varphi\right)\\&-\left(M_C+2M_W\right)g\sin\varphi\\&+M_Cl\dot{\theta}_C^{\,2}\sin\left(\theta_C+\varphi\right)\\\left(M_Cl^2+I_C\right)\ddot{\theta}_C=&-\left(T_L+T_R\right)+M_Cgl\sin\theta_C\\&-M_C\ddot{X}l\cos\left(\theta_C+\varphi\right)\\\ddot{\delta}=&\frac{\left(T_L-T_R\right)dr}{\left(M_Wd^2r^2+I_Wd^2+2I_Yr^2\right)}\end{aligned}\tag{14}$$

III. State Space Representation

A. Prepare for State Assignment

By substituting Eq. (10) into Eq. (8) and making some arrangements, one can obtain that

$$\begin{aligned}\ddot{X}=&\left(M_Cl^2+I_C\right)M_Clr^2\dot{\theta}_C^{\,2}\sin\left(\theta_C+\varphi\right)\\&-\left(M_Cl^2+I_C\right)\left(M_C+2M_W\right)gr^2\sin\varphi\\&\frac{-M_C^{\,2}l^2r^2g\sin\theta_C\cos\left(\theta_C+\varphi\right)}{\left(2M_Wr^2+M_Cr^2+2I_W\right)\left(M_Cl^2+I_C\right)}\\&-M_C^{\,2}l^2r^2\cos^2\left(\theta_C+\varphi\right)\end{aligned}$$

$$+\frac{\begin{array}{c}\left(T_L+T_R\right)\left(M_C l^2+I_C\right)r\\ +\left(T_L+T_R\right)M_C lr^2\cos\left(\theta_C+\varphi\right)\end{array}}{\begin{array}{l}\left(2M_W r^2+M_C r^2+2I_W\right)\left(M_C l^2+I_C\right)\\ -M_C{}^2 l^2 r^2\cos^2\left(\theta_C+\varphi\right)\end{array}} \tag{15}$$

Similarly, by inserting Eq. (8) into Eq. (10) and making some arrangements, we can obtain the following conclusion:

$$\begin{aligned}\ddot{\theta}_C=&\left(2M_W r^2+M_C r^2+2I_W\right)M_C gl\sin\theta_C\\ &+M_C\left(M_C+2M_W\right)lr^2 g\sin\varphi\cos\left(\theta_C+\varphi\right)\\ &\frac{-M_C{}^2 l^2 r^2\dot{\theta}_C{}^2\sin\left(\theta_C+\varphi\right)\cos\left(\theta_C+\varphi\right)}{\left(2M_W r^2+M_C r^2+2I_W\right)\left(M_C l^2+I_C\right)}\\ &-M_C{}^2 l^2 r^2\cos^2\left(\theta_C+\varphi\right)\\ &\left(2M_W r^2+M_C r^2+2I_W\right)\left(T_L+T_R\right)\\ &-\frac{+M_C lr\cos\left(\theta_C+\varphi\right)\left(T_L+T_R\right)}{\left(2M_W r^2+M_C r^2+2I_W\right)\left(M_C l^2+I_C\right)}\\ &-M_C{}^2 l^2 r^2\cos^2\left(\theta_C+\varphi\right)\end{aligned} \tag{16}$$

Based on the structure of Eqs. (15) and (16), let

$$\begin{cases}\mu=2M_W r^2+M_C r^2+2I_W\\ \lambda=M_C l^2+I_C\\ \alpha=M_W d^2 r^2+I_W d^2+2I_Y r^2\\ \beta=M_C lr\end{cases} \tag{17}$$

B. Linearization

Because of the influence of φ, when the TWSBR system becomes stable on the slope, the tilt angle θ_C will not be identical to zero. Instead, θ_C will become a constant θ_r and we define the error about tilt angle denoted as e_3, as follows:

$$e_3=\theta_C-\theta_r \tag{18}$$

With Eq. (14), the balance point θ_r can be calculated as:

$$\theta_r=\arcsin\left[\frac{r\left(M_C+2M_W\right)\sin\varphi}{M_C l}\right] \tag{19}$$

We set the state variables as follows:

$$\begin{cases}x_1=X\\ x_2=\dot{X}\\ x_3=\theta_C-\theta_r\\ x_4=\dot{\theta}_C\\ x_5=\delta\\ x_6=\dot{\delta}\\ u_1=T_L\\ u_2=T_R\end{cases} \tag{20}$$

and set the balance point as:

$$x=\begin{bmatrix}x_1 & x_2 & x_3 & x_4 & x_5 & x_6\end{bmatrix}^{\mathrm{T}}=0 \tag{21}$$

Based on Eqs. (20) and (21), Eq. (14) can be arranged into

$$\begin{aligned}\dot{x}_1&=x_2\\ \dot{x}_2&=\lambda\beta r x_4{}^2\sin\left(x_3+\theta_r+\varphi\right)\\ &\quad-\lambda\left(M_C+2M_W\right)gr^2\sin\varphi\\ &\quad\frac{-\beta^2 g\sin\left(x_3+\theta_r\right)\cos\left(x_3+\theta_r+\varphi\right)}{\mu\lambda-\beta^2\cos^2\left(x_3+\theta_r+\varphi\right)}\\ &\quad+\frac{\lambda r+\beta r\cos\left(x_3+\theta_r+\varphi\right)}{\mu\lambda-\beta^2\cos^2\left(x_3+\theta_r+\varphi\right)}\left(u_1+u_2\right)\\ \dot{x}_3&=x_4\\ \dot{x}_4&=\mu M_C gl\sin\left(x_3+\theta_r\right)\\ &\quad+\beta\left(M_C+2M_W\right)rg\sin\varphi\cos\left(x_3+\theta_r+\varphi\right)\\ &\quad\frac{-\beta^2\sin\left(x_3+\theta_r+\varphi\right)\cos\left(x_3+\theta_r+\varphi\right)x_4{}^2}{\mu\lambda-\beta^2\cos^2\left(x_3+\theta_r+\varphi\right)}\\ &\quad-\frac{\mu+\beta\cos\left(x_3+\theta_r+\varphi\right)}{\mu\lambda-\beta^2\cos^2\left(x_3+\theta_r+\varphi\right)}\left(u_1+u_2\right)\\ \dot{x}_5&=x_6\\ \dot{x}_6&=\frac{dr}{\alpha}\left(u_1-u_2\right)\end{aligned} \tag{22}$$

From Eq. (21), if x_3 is small enough, one has the following approximations:

$$\sin x_3\approx x_3,\cos x_3\approx 1 \tag{23}$$

By solving Eqs. (22) and (23), we can further obtain

$$\cos\left(x_3+\theta_r+\varphi\right)=\cos\left(\theta_r+\varphi\right) \tag{24}$$

$$\sin\left(x_3+\theta_r\right)=x_3\cos\theta_r+\sin\theta_r \tag{25}$$

By applying Eqs. (24) and (25) into Eq. (22), the equations which are unrelated to the state variables of $\dot{x}_2$ and $\dot{x}_4$ can be derived as follows:

$$\frac{-\beta^2 g\cos\left(\theta_r+\varphi\right)\sin\theta_r}{\mu\lambda-\beta^2\cos^2\left(\theta_r+\varphi\right)}+\frac{-\lambda\left(M_C+2M_W\right)gr^2\sin\varphi}{\mu\lambda-\beta^2\cos^2\left(\theta_r+\varphi\right)} \tag{26}$$

$$\frac{\mu M_C gl\sin\theta_r}{\mu\lambda-\beta^2\cos^2\left(\theta_r+\varphi\right)}+\frac{\beta\left(M_C+2M_W\right)rg\sin\varphi\cos\left(\theta_r+\varphi\right)}{\mu\lambda-\beta^2\cos^2\left(\theta_r+\varphi\right)} \tag{27}$$

We put Eqs. (26) and (27) into the control input. The state space expression can be obtained as follows:

$$\dot{x}=A_1 x+B_1 u \tag{28}$$

The control input can be defined as

$$u=\begin{bmatrix} T_L+T_R+\eta_m \\ T_L+T_R \end{bmatrix} \tag{29}$$

wherein

$$\eta_m=-r\left(M_C+2M_W\right)g\sin\varphi \tag{30}$$

Using Eqs. (24), (25), (29), (30) and solving the state Eq. (22) of TWSBR, the matrix A_1 and matrix B_1 in the state space expression Eq. (28) can be derived as follows:

$$A_1=\begin{bmatrix} 0 & 1 & 0 & 0 & 0 & 0 \\ 0 & 0 & \dfrac{-\beta^2 g\cos\theta_r\cos\left(\theta_r+\varphi\right)}{\mu\lambda-\beta^2\cos^2\left(\theta_r+\varphi\right)} & 0 & 0 & 0 \\ 0 & 0 & 0 & 1 & 0 & 0 \\ 0 & 0 & \dfrac{\mu M_C gl\cos\theta_r}{\mu\lambda-\beta^2\cos^2\left(\theta_r+\varphi\right)} & 0 & 0 & 0 \\ 0 & 0 & 0 & 0 & 0 & 1 \\ 0 & 0 & 0 & 0 & 0 & 0 \end{bmatrix} \tag{31}$$

$$B_1=\begin{bmatrix} 0 & 0 \\ \dfrac{\lambda r+\beta r\cos\left(\theta_r+\varphi\right)}{\mu\lambda-\beta^2\cos^2\left(\theta_r+\varphi\right)} & 0 \\ 0 & 0 \\ -\dfrac{\mu+\beta\cos\left(\theta_r+\varphi\right)}{\mu\lambda-\beta^2\cos^2\left(\theta_r+\varphi\right)} & 0 \\ 0 & 0 \\ 0 & \dfrac{dr}{\alpha} \end{bmatrix} \tag{32}$$

IV. Simulation Results and Analysis

Based on the state space equation in Eq. (28), we design an LQR controller to control the TWSBR system. We set the parameters as in Table II.

TABLE II. Parameter Value

parameter	value
M_W	4 kg
M_C	15 kg
I_W	0.02 kg·m^2
I_C	1.68 kg·m^2
I_Y	0.5 kg·m^2
r	0.05 m
l	0.4 m
d	0.4 m
g	9.8 m/s^2
φ	$\pi/6$ rad

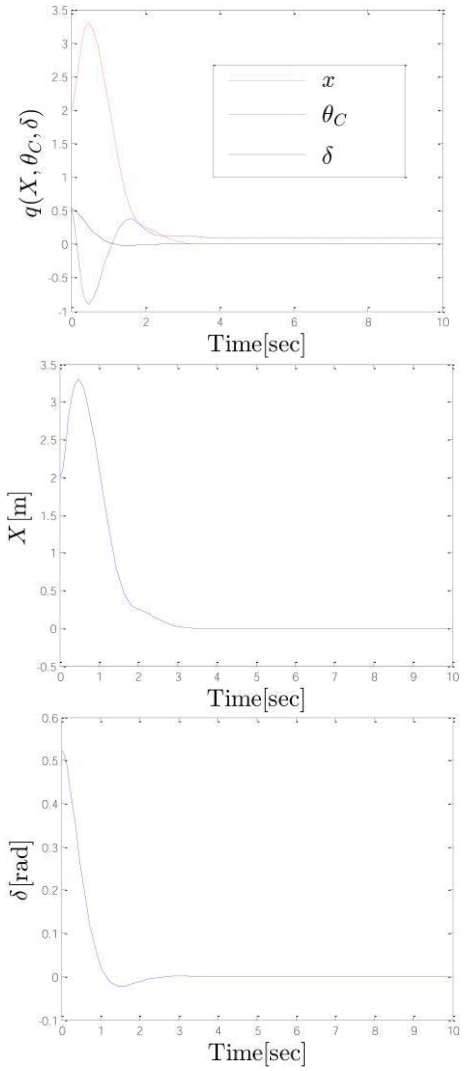

Fig. 3. The result figures of X,θ_C,δ.

We set Q as

$$Q=\begin{bmatrix} q_{11} & 0 & 0 & 0 & 0 & 0 \\ 0 & 0 & 0 & 0 & 0 & 0 \\ 0 & 0 & q_{33} & 0 & 0 & 0 \\ 0 & 0 & 0 & 0 & 0 & 0 \\ 0 & 0 & 0 & 0 & q_{55} & 0 \\ 0 & 0 & 0 & 0 & 0 & 0 \end{bmatrix} \tag{33}$$

and let R be selected as a second-order identity matrix. By using the way in [19] for parameter choosing, we finally choose $q_{11}=500, q_{33}=100, q_{55}=10$, and k is

$$k=\begin{bmatrix} -22.3607 & -20.9672 & -100.8804 & -26.3670 & 0 & 0 \\ 0 & 0 & 0 & 0 & 3.1623 & 1.5194 \end{bmatrix} \tag{34}$$

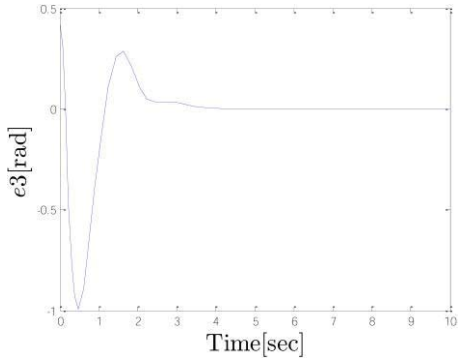

Fig. 4. The error figure of e_3 : e_3 is the difference of $\theta_C - \theta_r$.

In the simulation, the initial condition of TWSBR is set as

$$X = 2,\ \ \theta_C = \frac{\pi}{6},\ \ \delta = \frac{\pi}{6} \tag{35}$$

The simulation results are shown in Figs. 3 and 4. The steady-state error of X and the overshoot of θ_C are quite satisfactory in Fig. 3. The system reaches the steady status about 3 seconds without swinging. We can see e_3 converges to zero in Fig. 4 which validates the system can approach to the balance point Eq. (21) with the initial condition in Eq. (35).

V. Conclusions

This paper builds the dynamic equations of TWSBR systems on the slope. Further, the paper builds the system state space expression and designs the LQR controller to control the TWSBR on the slope. Some numerical simulation results are included for verification. In the future, we will carry out experiments on the hardware robot testbed.

References

[1] N. J. Nilsson, "Shakey the robot," *Stanford Research Institute Artificial Intelligence Center Technical Note*, no. 323, 1984.

[2] N. Sun, Y. Fang, and X. Zhang, "Energy coupling output feedback control of 4-DOF underactuated cranes with saturated inputs," *Automatica*, vol. 49, no. 5, pp. 1318-1325, May 2013.

[3] N. Sun and Y. Fang, "New energy analytical results for the regulation of underactuated overhead cranes: An end-effector motion-based approach," *IEEE Trans. Ind. Electron.*, vol. 59, no. 12, pp. 4723-4734, Dec. 2012.

[4] N. Sun, Y. Fang, Y. Zhang, and B. Ma, "A novel kinematic coupling-based trajectory planning method for overhead cranes," *IEEE/ASME Trans. Mechatronics*, vol. 17, no. 1, pp. 166-173, Feb. 2012.

[5] N. Sun, Y. Fang, and H. Chen, "A new antiswing control method for underactuated cranes with unmodeled uncertainties: Theoretical design and hardware experiments," *IEEE Trans. Ind. Electron.*, vol. 62, no. 1, pp. 453-465, Jan. 2015.

[6] N. Sun, Y. Fang, H. Chen, and B. He, "Adaptive nonlinear crane control with load hoisting/lowering and unknown parameters: Design and experiments," *IEEE/ASME Trans. Mechatronics*, vol. 20, no. 5, pp. 2107-2119, Oct. 2015.

[7] N. Sun, Y. Fang, X. Zhang, and Y. Yuan, "Transportation task-oriented trajectory planning for underactuated overhead cranes using geometric analysis," *IET Control Theory Appl.*, vol. 6, no. 10, pp. 1410-1423, Jul. 2012.

[8] N. Sun, Y. Fang, H. Chen, B. Lu, and Y. Fu, "Slew/translation positioning and swing suppression for 4-DOF tower cranes with parametric uncertainties: Design and hardware experimentation," *IEEE Trans. Ind. Electron.*, vol. 63, no. 10, pp. 6407-6418, Oct. 2016.

[9] N. Sun, Y. Fang, H. Chen, and B. Lu, "Amplitude-saturated nonlinear output feedback antiswing control for underactuated cranes with double-pendulum cargo dynamics," *Trans. Ind. Electron.*, in press.

[10] N. Sun, Y. Wu, Y. Fang, and H. Chen, "Nonlinear stabilization control of multiple-RTAC systems subject to amplitude-restricted actuating torques using only angular position feedback," *IEEE Trans. Ind. Electron.*, in press.

[11] N. Sun, Y. Wu, Y. Fang, H. Chen, and B. Lu, "Nonlinear continuous global stabilizing control for underactuated RTAC systems: Design, analysis, and experimentation," *IEEE/ASME Trans. Mechatronics*, in press.

[12] N. Sun and Y. Fang, "An efficient online trajectory generating method for underactuated crane systems," *Int. J. Robust Nonliner Control*, vol. 24, no. 11, pp. 1653-1663, 2014.

[13] K. Yamafuji, Y. Miyakuwa, and T. Kawamura, "Synchronous steering control of a parallel bicycle," *JSME*, vol. 55, no. 513, pp. 1229-1234, 1989.

[14] D. Voth, "Segway to the future [autonomous mobile robot]," *IEEE Intell. Syst.*, vol. 20, no.3, pp. 5-8, May/Jun., 2005.

[15] R. C. Ooi, "Balancing a two-wheeled autonomous robot [D]," Australia: University of Western Australia, 2003.

[16] K. DucDo and G. Seet, "Motion control of a two-wheeled mobile vehicle with an inverted pendulum," *J. Intell. Robot. Syst.*, vol. 60, no. 3–4, pp. 577–605, Dec. 2010.

[17] A. S. Katariya, "Optimal state-feedback and output-feedback controllers for the wheeled inverted pendulum system [D]," USA: Georgia Institue of Technology, 2010.

[18] J. X. Xu, Z. Q. Guo, and T. H. Lee, "Design and implementation of integral sliding mode control on an underactuated two-wheeled mobile robot," *IEEE Trans. Ind. Electron.*, vol. 61, no. 7, pp. 3671–3681, Jul. 2014.

[19] L. B. Prasad, B. Tyagi, and H.O. Gupta, "Optimal control of nonlinear inverted pendulum system using PID controller and LQR: performance analysis without and with disturbance input," *Int. J. Autom. Comput.*, vol. 11, no. 6, pp. 661–670, 2014.